AIP | Journal of Applied Physics

Planar metamaterial-based beam-scanning broadband microwave antenna

Abdallah Dhouibi, Shah Nawaz Burokur, and André de Lustrac

Citation: Journal of Applied Physics **115**, 194901 (2014); doi: 10.1063/1.4876233
View online: http://dx.doi.org/10.1063/1.4876233
View Table of Contents: http://scitation.aip.org/content/aip/journal/jap/115/19?ver=pdfcov
Published by the AIP Publishing

Planar metamaterial-based beam-scanning broadband microwave antenna

Abdallah Dhouibi,[1] Shah Nawaz Burokur,[1,2,a)] and André de Lustrac[1,2]
[1]IEF, CNRS, UMR 8622, Univ. Paris-Sud, 91405 Orsay Cedex, France
[2]Univ. Paris-Ouest, 92410 Ville d'Avray, France

(Received 21 March 2014; accepted 30 April 2014; published online 15 May 2014)

The broadband directive emission from the use of waveguided metamaterials is numerically and experimentally reported. The metamaterials, which are composed of non-resonant circular complementary closed ring structures printed on a dielectric substrate, are designed to obey the refractive index of a Luneburg lens. An arc array of planar radiating slot antennas placed at the periphery of the lens is used as wave launchers. A prototype of the lens associated with the feed structures has been fabricated using standard lithography techniques. To experimentally demonstrate the broadband focusing properties and directive emissions, far-field radiation patterns have been measured. Furthermore, this metamaterial-based lens can be used to achieve beam-scanning with a coverage of up to 120°. Far-field measurements agree qualitatively with calculated near-field distributions. © *2014 AIP Publishing LLC*. [http://dx.doi.org/10.1063/1.4876233]

I. INTRODUCTION

Artificial subwavelength composite materials referred to as metamaterials are typically fabricated via a suitable periodic arrangement of micro-structured metallic or dielectric inclusions. Their unusual electromagnetic properties have made relevant a wide array of interesting applications particularly since the introduction of the transformation optics concept.[1,2] Devices, such as invisibility cloaks,[3–5] directive[6] and omnidirectional[7,8] antennas, Luneberg[9] and Eaton[10] lenses, and waveguide tapers,[11] have then been proposed. The implementation of such devices is generally achieved using materials presenting permittivity and/or permeability gradients, which can be provided by metamaterial engineering. In recent few years, gradient index (GRIN) metamaterials having the ability to deflect a propagating beam have been used as lenses.[12] These lenses where the refractive index varies linearly are alternatives to conventional dielectric ones that rely on the interfaces of the dielectric material to control light flow. As such, cylindrical waves propagating through a well-designed planar gradient index lens can be transformed to plane waves. The attractive performances of lens antennas[13] for radio frequency (RF) communications have then been highlighted.

Experimental validation of such GRIN lenses showing good efficiencies has been reported recently.[14–25] For example, a three-dimensional (3D) version of the two-dimensional (2D) flattened Luneburg lens of Ref. 9 has been experimentally demonstrated.[18] The GRIN lenses presented in Refs. 15, 16, and 22–24 have been constructed in a parallel-plate quasi-transverse electromagnetic (TEM) waveguide configuration by utilizing a 2D metamaterial that is able to support bulk electromagnetic modes. Recently, we have experimentally validated the integration of a planar wave launcher to feed the lens in order to achieve a planar broadband lens antenna, thus facilitating its integration in RF communication systems.[22–24]

In this study, we design a 2D planar and electrically compact Luneburg lens operating in the [8 GHz–12 GHz] frequency band, using GRIN metamaterials. The gradient index of the lens is achieved through a two-dimensional array of waveguided building blocks of complementary closed ring (CCR) resonators. We focus our attention on the combination of multiple planar antennas used as wave launchers to feed the lens in the parallel-plate waveguide. By switching between the feed antenna elements, beam scanning from −60° to +60° is successfully realized. The proposed lens antenna configuration offers advantages of compact, low profile, lightweight, and broadband features and also easy fabrication. Reported experimental far-field radiation patterns demonstrate broadband directive and steerable emissions, validating the good efficiency of the planar metamaterial-based GRIN lens antenna. Parallel recent studies have approached 20° beam scanning from a metasurface lens designed through the use of transformation optics concept.[26]

II. BROADBAND METAMATERIAL CELLS

A broadband metamaterial-based Luneburg lens of radius $R = 57.4$ mm is designed to operate in the 8 GHz to 12 GHz frequency band. A circular non-resonant magnetic CCR waveguided structure is used as the basic building block to design the artificial medium representing the lens. The circular closed ring resonators are etched on the copper-cladding of a 1.6 mm thick Rogers RT/duroid® 5880 substrate, ($\varepsilon_r = 2.2$ and $\tan\delta = 0.0009$). In contrast to our previous works,[22–24] here we favor for a circular ring design due to its symmetry and therefore to its incidence-independency characteristics. Such a complementary resonator operates in a quasi-TEM waveguide configuration as shown in Fig. 1(a) and exhibits a magnetic resonance when the E-field is aligned perpendicularly to its plane. To obtain the desired effective index of the CCR units, the properties are characterized numerically using Maxwell's equations solver of CST Microwave Studio Suite. The polarization of the incident

a)shah-nawaz.burokur@u-psud.fr

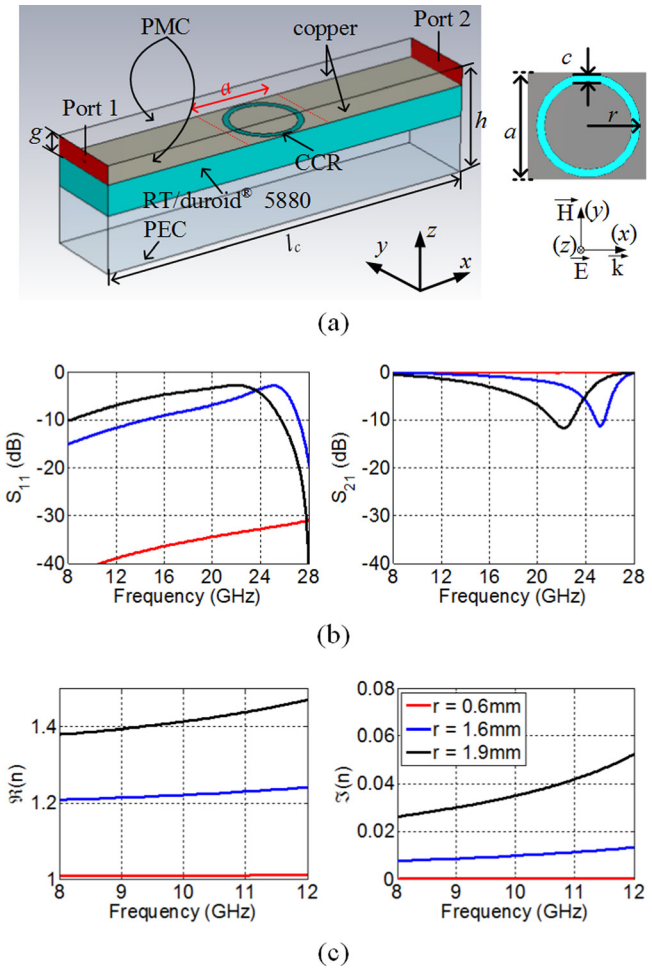

FIG. 1. (a) Simulation setup used to retrieve the effective constitutive parameters of the CCR cells. (b) Reflection and transmission responses of a typical CCR structure with varying r values, which is used in the non-resonant frequency regime such that it presents broadband features in the 8–12 GHz band (less than 7% variation over the whole band). (c) Extracted effective index of the CCR structure. The geometrical dimensions are $l_c = 20$ mm, $h = 5.6$ mm, $g = 1$ mm, $a = 4.1$ mm, and $c = 0.3$ mm.

TEM wave is constrained by the use of perfect magnetic conducting (PMC) boundaries on the sides of the computational domain in the xz plane. The gap g between the patterned circuit board and the top copper plate of the waveguide is fixed to 1 mm. Radiation boundaries are assigned below the ports in the yz plane. The two ports are placed far away from the resonator structure to avoid near-field cross coupling between the ports and the CCR. However, the phase reference planes for the electromagnetic parameters retrieval are chosen such that the period a of the CCR unit cell is kept as 4.1 mm. The variation of the refractive index from $\sqrt{2}$ at the center to 1 on the border of the lens consists in changing the CCR radius r, while keeping the other geometrical parameters fixed. In our design, the Luneburg lens is discretized into seven concentric regions, where each region composed of two cells corresponds to a specific refractive index. The 1 and $\sqrt{2}$ index value regions correspond, respectively, to $r = 0.6$ mm and $r = 1.9$ mm. The electromagnetic parameters are retrieved using the simulated S-parameters as proposed by the inversion method described in Ref. 27.

The reflection and transmission characteristics of the waveguided CCR metamaterials are shown for three different r values in Fig. 1(b). As r increases, the resonance frequency decreases. Fig. 1(c) shows the real and imaginary parts of the effective index (n_{eff}) extracted from the complex reflection and transmission coefficients. They are used in their non-resonant frequency regime such that they present broadband material properties in the 8–12 GHz band. Indeed, for frequencies well below resonance, the structure behaves as an effective medium. We can observe that the index presents low dispersion even for $r = 1.9$ mm in which case resonance is around 22 GHz. Far from resonance, losses are found to be very low as illustrated by the imaginary parts in Fig. 1(c).

III. DESIGN OF THE METAMATERIAL-BASED LENS ANTENNA

The planar lens constructed from the waveguided CCR building blocks is inserted in a quasi-TEM waveguide consisting of two circular parallel copper plates spaced by $h = 5.6$ mm, consistent to the simulation setup of the CCR cell. As shown in Fig. 2, the GRIN slab is placed on a Rohacell® foam spacer, with a relative permittivity close to 1, to fill up the space between the lens and the bottom metallic plate. The effective refractive index can be varied from 1.01 to 1.41 by varying the radius of the CCR cell from

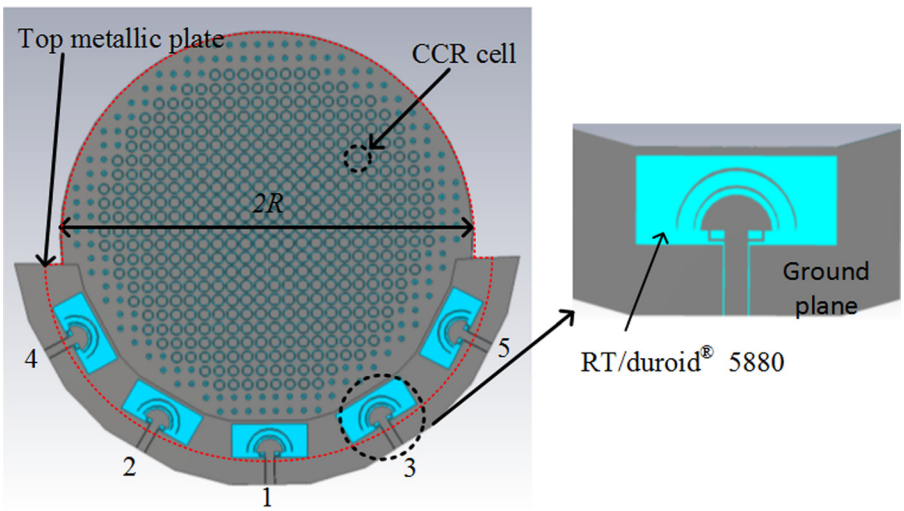

FIG. 2. Schematic view of the lens antenna composed of a planar metamaterial-based lens and radiating slot elements placed in a quasi-TEM parallel-plate waveguide. The radius of the lens is $R = 57.4$ mm.

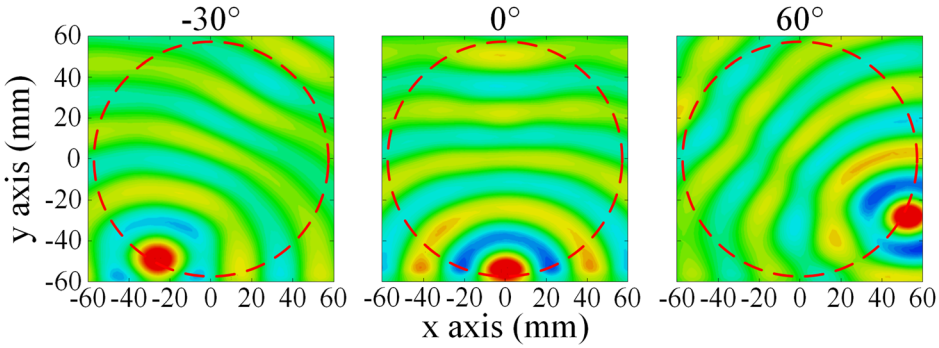

FIG. 3. Calculated electric near-field distribution at 10 GHz for three different excited sources, illustrating the beam-scanning performances of the metasurface used as lens.

0.6 mm to 1.9 mm in the seven discretized regions of the lens. An arc array of five planar microstrip antennas partially inserted in the parallel-plate waveguide and placed at the periphery of the lens is used as primary feeds. As shown by the inset of Fig. 2, each antenna element is composed of rectangular radiating slot milled on a similar substrate as the Luneburg lens. The slot is excited by a 50 Ω coplanar waveguide line ended with a radial stub. Two arc conducting lines are printed on the radiating slot in order to improve the impedance matching of the antenna element. It should be noted that only the radiating slot of the feed is inserted between the parallel plate waveguide. The coplanar waveguide line exciting the slot is kept outside the quasi-TEM waveguide. Such a configuration facilitates matching of the antenna element. The antenna elements with angular interval of 30° of the feeding array are positioned such that the phase center is situated at the lens periphery. The feeding structure is designed to provide an electric field parallel to the z-axis and perpendicular to the CCR plane. The dominant TEM mode is formed between the top metallic plate of the quasi-TEM waveguide and the CCR-based lens.

To verify the beam-scanning of the designed Luneburg lens at 10 GHz, calculated near-field distributions of the z-component of the electric field (E_z) above the lens are presented in Fig. 3 for the excited feeding sources numbered "1," "2," and "5." The incident waves radiated by the radiating slot feed pass through the metasurface region with low reflections as shown by the near field distributions. As illustrated, while passing through the lens region (shown by the dashed red trace), the circular wavefronts radiated from the feed are flattened and the cylindrical waves are gradually transformed into quasi-plane waves, demonstrating a highly directive radiation on the opposite side of the lens. By switching among the several feeds around the lens, propagation direction changes as shown in Fig. 3, indicating the good beam-scanning performances of the lens antenna.

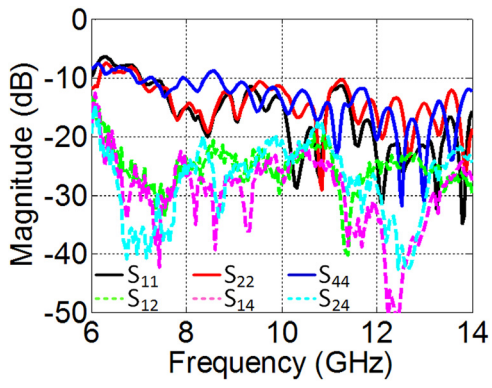

FIG. 4. Measured S_{ij} parameters of the lens antenna showing good matching and high isolation.

IV. EXPERIMENTAL VALIDATION OF BEAM SCANNING

To validate experimentally the concept, a prototype has been fabricated and tested. The impedance matching of the lens antenna is illustrated by the measured reflection coefficient shown in Fig. 4. A relatively good matching (<-9 dB) is observed experimentally in the [8 GHz –12 GHz] frequency band. The coupling between the different feed elements is also given in the Fig. 4 and shows an average value of −20 dB over the whole frequency band, indicating a very good isolation.

To investigate the directive behavior and beam scanning performances of the integrated lens antenna, far-field radiation patterns have been measured in a full anechoic chamber. When the feeding elements "1," "2," and "5" are independently excited, the measured radiation patterns at 8, 10, and 12 GHz are presented in Figs. 5(a)–5(c). A highly directive

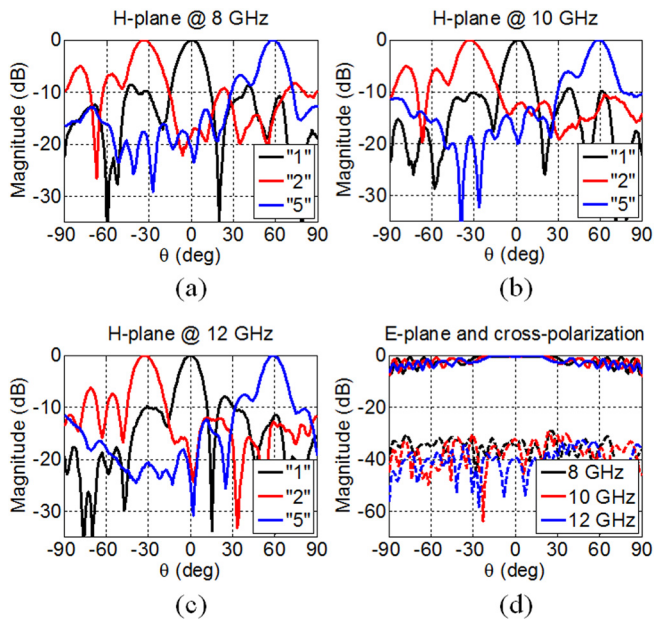

FIG. 5. Measured co-polarization and cross-polarization far-field components at 8, 10, and 12 GHz. (a)–(c) H-plane when sources "1," "2," and "5" are excited. (d) E-plane (—) and cross-polarization (- - -) when source "1" is excited.

radiated lobe is observed in the H-plane (plane containing H and k vectors) at all tested frequencies. By switching between the feeding sources, beam scanning can therefore be achieved from $-60°$ to $+60°$. The measured half-power beam width is less than 18° in the whole operating frequency band and whole angle scanning coverage. The measured side lobes are around −6 dB for the worst case due to the relatively small radius of the lens ($<2\lambda_0$ at 10 GHz). A larger radius should lead to lower parasitic lobes. As presented in Fig. 5(d) for normal radiated beam when feed "1" is excited, a wide beam is radiated in the E-plane (plane containing E and k vectors), resulting in a three-dimensional fan-shaped beam of the lens antenna. The cross-polarization components measured show levels remaining below −29 dB over the whole [8 GHz–12 GHz] frequency band. The measured directivity of the proposed lens antenna is found to lie between 14 dBi and 15 dBi in the frequency range of interest for both broadside and off-normal emissions.

V. CONCLUSIONS

In summary, we have experimentally validated a substrate-integrated planar Luneburg lens that presents high beam-scanning performances with a coverage of 120° over a wide frequency range in the microwave region. The metamaterial-based structure is excited by an array of planar radiating slots placed on its periphery and is configured to operate in a quasi-TEM parallel-plate waveguide. The near-field distributions have demonstrated a directive emission obtained by the transformation of cylindrical waves into quasi-plane waves, and the association between the feed structure and the metamaterial-based lens has shown a broadband frequency operation from 8 GHz to 12 GHz.

ACKNOWLEDGMENTS

This work was supported by the EADS Company Foundation through the METAQOPT project, Contract No. 090-AO09-1006. One of the authors (A.D.) would like to acknowledge support for his Ph.D. scholarship from EADS Company Foundation.

[1]U. Leonhardt, Science **312**, 1777 (2006).
[2]J. B. Pendry, D. Schurig, and D. R. Smith, Science **312**, 1780 (2006).
[3]D. Schurig, J. J. Mock, B. J. Justice, S. A. Cummer, J. B. Pendry, A. F. Starr, and D. R. Smith, Science **314**, 977 (2006).
[4]W. Cai, U. K. Chettiar, A. V. Kildishev, and V. M. Shalaev, Nat. Photonics **1**, 224 (2007).
[5]B. Kanté, A. de Lustrac, J.-M. Lourtioz, and S. N. Burokur, Opt. Express **16**, 9191 (2008).
[6]P.-H. Tichit, S. N. Burokur, D. Germain, and A. de Lustrac, Phys. Rev. B **83**, 155108 (2011).
[7]P.-H. Tichit, S. N. Burokur, and A. de Lustrac, Opt. Express **19**, 20551 (2011).
[8]P.-H. Tichit, S. N. Burokur, C.-W. Qiu, and A. de Lustrac, Phys. Rev. Lett. **111**, 133901 (2013).
[9]N. Kundtz and D. R. Smith, Nature Mater. **9**, 129 (2010).
[10]Y. G. Ma, C. K. Ong, T. Tyc, and U. Leonhardt, Nature Mater. **8**, 639 (2009).
[11]P.-H. Tichit, S. N. Burokur, and A. de Lustrac, Opt. Express **18**, 767 (2010).
[12]D. R. Smith, J. J. Mock, A. F. Starr, and D. Schurig, Phys. Rev. E **71**, 036609 (2005).
[13]T. Driscoll, D. N. Basov, A. F. Starr, P. M. Rye, S. Nemat-Nasser, D. Schurig, and D. R. Smith, Appl. Phys. Lett. **88**, 081101 (2006).
[14]H. F. Ma, X. Chen, H. S. Xu, X. M. Yang, W. X. Jiang, and T. J. Cui, Appl. Phys. Lett. **95**, 094107 (2009).
[15]Q. Cheng, H. F. Ma, and T. J. Cui, Appl. Phys. Lett. **95**, 181901 (2009).
[16]C. Pfeiffer and A. Grbic, IEEE Trans. Antennas Propag. **58**, 3055 (2010).
[17]H. F. Ma, X. Chen, X. M. Yang, H. S. Xu, Q. Cheng, and T. J. Cui, Chin. Sci. Bull. **55**, 2066 (2010).
[18]H. F. Ma and T. J. Cui, Nat. Commun. **1**, 124 (2010).
[19]X. Chen, H. F. Ma, X. Y. Zou, W. X. Jiang, and T. J. Cui, J. Appl. Phys. **110**, 044904 (2011).
[20]Z. L. Mei, J. Bai, T. M. Niu, and T. J. Cui, IEEE Trans. Antennas Propag. **60**, 398 (2012).
[21]Y. L. Loo, Y. Yang, N. Wang, Y. G. Ma, and C. K. Ong, J. Opt. Soc. Am. A **29**, 426 (2012).
[22]A. Dhouibi, S. N. Burokur, A. de Lustrac, and A. Priou, IEEE Antennas Wireless Propag. Lett. **11**, 1504 (2012).
[23]A. Dhouibi, S. N. Burokur, A. de Lustrac, and A. Priou, IEEE Antennas Wireless Propag. Lett. **12**, 43 (2013).
[24]A. Dhouibi, S. N. Burokur, A. de Lustrac, and A. Priou, Appl. Phys. Lett. **102**, 024102 (2013).
[25]J. A. Dockrey, M. J. Lockyear, S. J. Berry, S. A. R. Horsley, J. R. Sambles, and A. P. Hibbins, Phys. Rev. B **87**, 125137 (2013).
[26]X. Wan, W. X. Jiang, H. F. Ma, and T. J. Cui, Appl. Phys. Lett. **104**, 151601 (2014).
[27]D. R. Smith, S. Schultz, P. Markos, and C. M. Soukoulis, Phys. Rev. B **65**, 195104 (2002).